



# Cytologic and Molecular Assessment of Isthmus Thyroid Nodules and Carcinomas

Sina Jasim,<sup>1</sup> Allan Golding,<sup>2</sup> David Bimston,<sup>2</sup> Mohammed Alshalalfa,<sup>3</sup> Yang Chen,<sup>3</sup> Ruochen Jiang,<sup>3</sup> Yangyang Hao,<sup>3</sup> Jing Huang,<sup>3</sup> Joshua P. Klopper,<sup>3</sup> Richard T. Kloos,<sup>3</sup> and Taylor C. Brown<sup>1</sup>

**Background:** Isthmic thyroid nodules are more likely to be malignant and isthmic differentiated thyroid cancer demonstrates less favorable behavior compared with lobar locations. The goal of this study was to assess molecular differences of thyroid nodules and carcinomas from the isthmus relative to the lobes.

**Methods:** The Afirma thyroid nodule database ( $n = 177,227$ ) was assessed for cytologic and molecular differences between isthmus and lobar nodules in this observational cohort study. Genome-wide differential expression analysis was conducted to decipher transcriptomic differences. Histopathology reports ( $n = 583$ ) of papillary thyroid cancer (PTC) ( $n = 389$ ) and infiltrative follicular subtype of PTC (IF-PTC) ( $n = 194$ ) from Afirma discovery cohorts and from thyroid cancer patients managed at an integrative endocrine surgery community care practice were analyzed for molecular differences between isthmic and lobar cancers.

**Results:** In the Afirma database, 8527 (4.8%) isthmus nodules were identified. Bethesda V–VI nodules were almost twice as prevalent from the isthmus as compared with the lobes (8.2% vs. 4.3%,  $p < 0.0001$ ). Isthmus nodules had twice the frequency of *BRAF*<sup>V600E</sup> (21% vs. 10.6%,  $p < 0.0001$ ), an increased frequency of *ALK/NTRK/RET* fusions (4.6% vs. 2.5%,  $p < 0.0001$ ) and *SPOP* variants (1.5% vs. 0.8%,  $p < 0.0001$ ), and a lower frequency of *NRAS* mutations (7.8% vs. 13.2%,  $p < 0.0001$ ), and *PAX8::PPAR $\gamma$*  fusions (1.1% vs. 2.3%,  $p < 0.0001$ ) than lobar nodules. Transcriptome analysis of molecular signatures and genome-wide analysis showed that isthmus nodules have higher *BRAF*-like scores, ERK activity, follicular mesenchymal transition scores (FMT), and lower inflammation activity scores. Pathway enrichment analysis revealed genes downregulated in isthmus tumors are enriched in immune response regulation. IF-PTC from the isthmus ( $n = 13$ ) were more *BRAF*-like and had increased ERK and FMT scores compared with those from the lobes ( $n = 181$ ) ( $p < 0.01$  for all).

**Conclusions:** These data suggest isthmic nodules are more likely to have malignant cytology and increased rates of higher risk molecular alterations compared with lobar nodules. IF-PTC from the isthmus is molecularly different compared with IF-PTC from the lobes. More data are needed to know if a change in surgical therapy is warranted in isthmic thyroid cancers relative to lobar cancers and if this molecular data should influence isthmic thyroid cancer management and monitoring.

**Keywords:** thyroid isthmus, Afirma, molecular diagnostics, thyroid nodule, thyroid cancer

## Introduction

The thyroid isthmus is normally a thin piece of tissue that lies anterior to the trachea and connects the two lobes of the thyroid. Thyroid nodules are very common with over 60% of the population having one or more by the seventh and eighth decades of life.<sup>1</sup> Isthmic thyroid nodules are

detected about eight times less frequently than nodules in the lobes.<sup>2</sup> However, recent studies have shown that the risk of malignancy arising from isthmic thyroid nodules is greater than lobar nodules.<sup>2,3</sup> In addition, isthmic thyroid cancers have been shown to exhibit more aggressive behavior compared to lobar thyroid cancers, including higher rates of extrathyroidal extension, capsular invasion, and lymph node

<sup>1</sup>Washington University School of Medicine in St. Louis, St. Louis, MO, USA.

<sup>2</sup>Memorial Healthcare System, Hollywood, FL, USA.

<sup>3</sup>Veracyte, Inc., South San Francisco, CA, USA.

metastasis.<sup>4,5</sup> Though the anatomical location, thin tissue approximating the thyroid capsule, and unique lymphatic drainage<sup>6–8</sup> have been noted as reasons for worse pathological features, molecular differences were shown in isthmus papillary thyroid carcinoma (PTC) with higher ERK and lower thyroid differentiation scores (TDSs) compared with lobar PTC.<sup>9</sup>

Approximately 20–25% of thyroid nodule aspirates result in The Bethesda System for Reporting Thyroid Cytopathology Bethesda (B) III or IV cytology (together, indeterminate thyroid nodules [ITN]).<sup>10</sup> The risk of malignancy of ITN ranges from 13–34% depending on the institution and the categorization of noninvasive follicular thyroid neoplasm with papillary-like nuclear features) as benign or malignant.<sup>11</sup> To help address the clinical challenge of ITN, the Afirma Gene Expression Classifier (GEC) was developed and eventually replaced by the Afirma Genomic Sequencing Classifier (GSC) after clinical and analytical validation.<sup>12,13</sup> The Afirma GSC uses exome-enriched RNA sequencing (RNAseq) such that each sample is sequenced for 26,268 genes, providing data on gene and exon expression, mitochondrial expression, loss of heterozygosity, and detection of expressed gene variants and fusions.<sup>14</sup> Therefore, Afirma testing can clinically provide both diagnostic (in ITN) and prognostic information in BIII–VI thyroid nodule<sup>15</sup> and be analyzed for gene expression signatures and biological pathways as a research tool.

The purpose of this study was to interrogate the Afirma thyroid nodule database (AfirmaDB) to assess the cytological and molecular differences between thyroid nodules of the isthmus and lobes. In addition, a cohort of thyroid cancers that underwent Afirma testing were analyzed to assess for histological, molecular, clinicopathologic outcome differences between isthmus and lobar thyroid carcinoma.

## Materials and Methods

### Thyroid nodule evaluation

Analysis of 177,227 consecutive thyroid nodules with clinical Afirma GSC results from 2017 to 2022 with BIII–VI cytology by location (as indicated on the test request form, isthmus vs. non-isthmus [lobar]), cytology category (BIII–IV vs. BV–VI), sex, age, and Genomic Sequencing Classifier-Suspicious (GSC-S) rate was performed in this observational cohort study (Fig. 1 and Table 1). Most nodules referred had BIII and BIV cytology and were analyzed to assess if these nodules were molecularly benign and could avoid unnecessary surgery.<sup>16</sup> Cytology was read either at a local pathology practice or, when preferred, at Thyroid Cytopathology Partners (Austin, TX). There was no formal centralized cytopathology review. The relative frequencies of genomic alterations (variants and fusions) from the Afirma Xpression Atlas<sup>17</sup> were evaluated by nodule location across different subgroups (ITN GSC-S and BV–VI combined, ITN GSC-S and BV–VI alone) and without knowledge of the final histopathology when applicable.

### Thyroid carcinoma evaluation

Local histopathology reports from differentiated thyroid carcinoma (DTC) (infiltrative follicular subtype of papillary

thyroid carcinoma ([IF-PTC]) = 194, PTC = 389) from Afirma GSC discovery/training cohorts<sup>13</sup> ( $n = 251$  collected from 2013 to 2016) and from thyroid cancer patients managed at an integrative endocrine surgery community care practice (Memorial Healthcare System,  $n = 332$  collected from August 2017 to July 2022) that all underwent Afirma GSC exome-enriched RNAseq analysis were assessed for cytological differences and gene expression signatures based on cancer location.<sup>13</sup> Memorial Healthcare submitted thyroid nodule biopsy specimens with BIII–VI cytology (with local cytopathology reads) for Afirma testing in an actively managed cohort, from which molecular findings were correlated to final histopathology (Fig. 1).

### Biological pathways enrichment analysis

For molecular difference assessment, 54 gene expression signatures were evaluated. These include activity scores of 50 hallmarks of cancer pathways,<sup>18</sup> *BRAF*-like to *RAS*-like molecular score (BRS), ERK signaling, TDS and follicular to mesenchymal transition score (FMT). For pathway enrichment analysis, transcriptome-wide differential expression analysis using 26,268 genes was conducted to identify genes upregulated and downregulated in isthmus nodules by using Wilcoxon rank sum statistical test. g:Profiler online tool (<https://biit.cs.ut.ee/gprofiler/gost>) was used to identify biological pathways enriched in upregulated and downregulated genes in isthmus nodules.<sup>19</sup> EnrichmentMap and Cytoscape tools were used to take g:Profiler output and build a network of related, significantly enriched pathways.<sup>20,21</sup> Finally, to gain more insights into the immune content of the sequenced samples, we used ESTIMATE algorithm that uses deconvolution of bulk gene expression data to output estimated levels of infiltrating immune cells.<sup>22</sup>

### Institutional review board approval

The Afirma GSC discovery cohort pathology reports were from subjects recruited for the Afirma GEC and subsequent GSC training and validation studies with approval of institutional-specific review boards, Chesapeake IRB (now Advarra IRB, Columbia, MD), and Copernicus Group Independent Review Board (now WCG IRB, Princeton, NJ).<sup>13</sup> Patients recruited to the Afirma GEC validation study provided written informed consent.<sup>12</sup> Memorial health patient data, including cytology and histopathology reports, was collected under WCG IRB protocol # DHF 005-044.

### Statistical analysis

All statistical analyses were conducted in R 3.2. Wilcoxon rank sum test was used to assess differences of continuous variables (gene expression, pathway scores, *BRAF*-like score, ERK, FMT) between nodule locations and for genome-wide differential expression analysis. The chi-square test was used to assess significant associations between cytology groups, genomic alterations, and nodule location. Logistic regression was used to calculate odd ratios (ORs) of cancer pathway scores and their association with isthmus nodules. Multiple testing  $p$  value correction was done using Benjamini-Hochberg procedure.

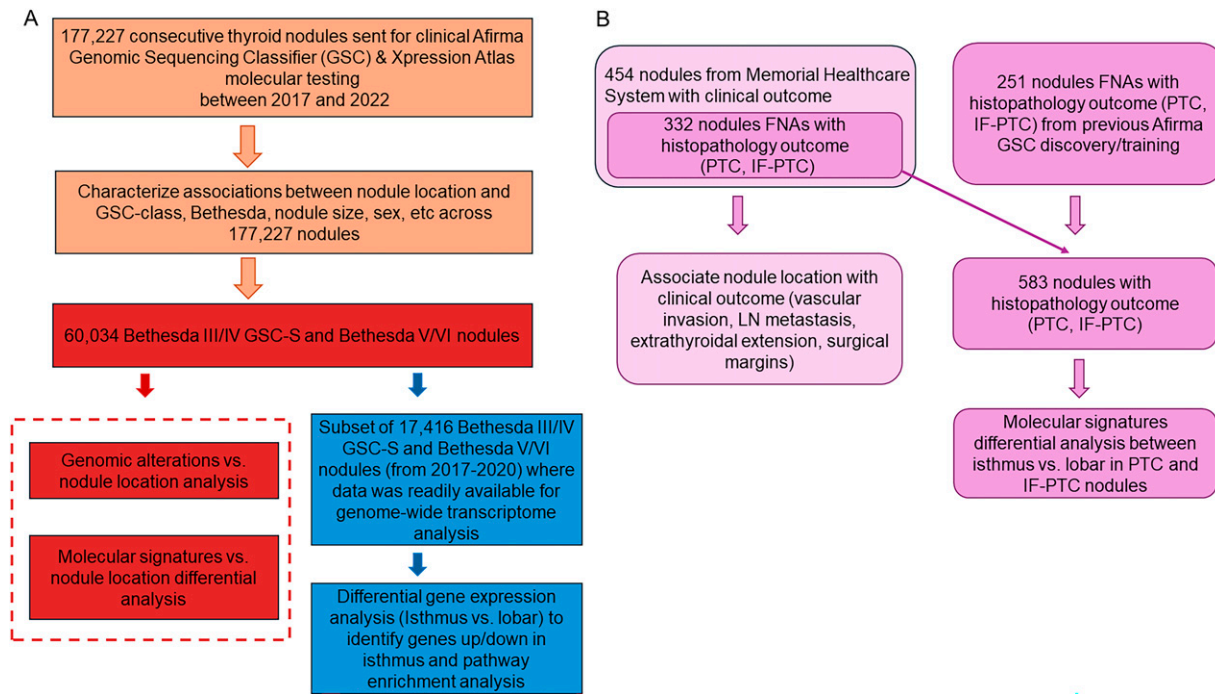


**FIG. 1.** Flowchart of cohorts used, and analyses conducted. **(A)** A total of 177,227 samples with nodule location were extracted from AfirmaDB. Initial analysis was conducted to associate nodule location with other clinical variables across all samples. Nodule size was broken into multiple groups; (x, y) includes the nodules  $\geq x$  and  $< y$  cm. Associating genomic alterations with nodule location was conducted in Bethesda III/IV samples classified as GSC-suspicious or Bethesda V/VI samples (total  $n = 60,034$ ). Whole genome-transcriptomic analysis was conducted on the early samples ( $n = 17,416$ ) sent for molecular testing between 2017 and 2020. **(B)** Two cohorts were used for associating nodule location with clinical and pathology outcomes. A subset of 332 samples, with IF-PTC or PTC pathology, from Memorial Healthcare System were pooled with 251 samples from previous Afirma training cohort to characterize molecular differences between isthmus and lobar nodules with different pathology outcomes. AfirmaDB, Afirma thyroid nodule database; GSC, genomic sequencing classifier; IF-PTC, infiltrative follicular subtype of PTC; PTC, papillary thyroid cancer.

## Results

A total of 177,227 nodules were evaluated with 8527 from the isthmus (4.8%) (Table 1). The median age was slightly higher in patients with lobar nodules (57.7 vs. 59 years old,  $p < 0.001$ ). More female patients were found with isthmus nodules compared with lobar nodules (80% vs. 77.4%,  $p < 0.001$ ). Isthmus nodules were twice as likely to have BV–VI cytology compared with lobar nodules (8.2% vs. 4.3%,  $p < 0.001$ ). There was no significant difference in the GSC-S call rate of isthmus versus lobar nodules for ITN (30.5% vs. 30.8%,  $p = 0.52$ ) (Table 1).

Genomic analysis within ITN GSC-S or BV–VI nodules showed that isthmus nodules were more enriched with molecular variants and fusions at high-risk for malignancy like *BRAFp.V600E* (21% vs. 10.6%,  $p < 0.0001$ ) and *ALK/NTRK/RET* fusions (4.5% vs. 2.5%,  $p < 0.0001$ ) (Table 2). Additionally, *SPOP* variants were statistically more frequent in the isthmus (1.5% vs. 0.75%,  $p < 0.0001$ ). Moderate risk for malignancy variants that were overrepresented in the lobes relative to the isthmus were: *NRAS* (13.2% vs. 7.9%,  $p < 0.0001$ ), *HRAS* (8.3% vs. 4.6%,  $p < 0.0001$ ), and *PAX8::PPARy* fusions (2.3% vs. 1.1%,  $p < 0.0001$ ). In addition, *RET* variants were overrepresented in the lobes relative to the isthmus (0.53% vs. 0.06%,  $p = 0.001$ ). Genomic analysis of ITN GSC-S nodules alone showed a similar trend of

overrepresentations of *BRAFp.V600E*, *ALK/NTRK/RET* fusions, and *SPOP* variants in isthmus nodules (Table 2).

To further gain molecular insights into the differences between isthmus and lobar nodules, we evaluated 54 gene expression-based signatures that are thyroid specific BRS, ERK activity, FMT, TDS, and pan-cancer (Molecular Signatures Database hallmarks of cancer pathways) (Fig. 2). Within ITN GSC-S and B V–VI subgroups, isthmus nodules had significantly higher BRS score, ERK activity, and FMT scores ( $p < 0.0001$  for all). Differential analysis of cancer hallmark pathways scores showed that isthmus nodules have higher scores of epithelial-mesenchymal transition (EMT), coagulation, apical junctions, angiogenesis, estrogen receptor, and TGF-beta signaling. However, they had lower activity of PI3K-AKT signaling, heme metabolism and inflammation immune related signatures (Fig. 2). The same trend was observed for the 54 signatures when limiting the analysis to ITN GSC-S samples or *BRAF*-negative ITN GSC-S and BV–VI samples. (Supplementary Figures S1-S2).

Transcriptome-wide differential expression analysis showed that 1619 genes were found upregulated in lobar, and 1329 genes were upregulated in isthmus nodules within ITN GSC-S and BV/VI samples (Fig. 3). To gain functional insights into these genes, we conducted gene set enrichment analysis using g:Profiler online tool to identify biological pathways enriched in upregulated genes in isthmus and lobar nodules.<sup>19</sup>



TABLE 1. CHARACTERISTICS OF SAMPLES FROM AFIRMADB WITH NODULE LOCATION

	Isthmus	Lobar	p value
Total	8527	168,700	
Age (median [IQR])	57.7 (45.6–68.1)	59.1 (46.3–69.2)	<0.0001
Sex			<0.0001
Male	1701 (19.95%)	38,151 (22.62%)	
Female	6826 (80.05%)	130,549 (77.38%)	
Nodule size			<0.0001
Median (IQR)	1.9 (1.4–2.6)	2.2 (1.6–3.1)	
<1 cm	338 (3.96%)	4452 (2.64%)	
(1–2 cm)	4098 (48.06%)	63,879 (37.86%)	
(2–3 cm)	2626 (30.8%)	49,882 (29.57%)	
(3–4 cm)	975 (11.43%)	27,305 (16.19%)	
≥4 cm	467 (5.48%)	22,792 (13.5%)	
Bethesda			<0.0001
III	6284 (73.7%)	132,961 (78.82%)	
IV	1544 (18.1%)	28,568 (16.93%)	
V	278 (3.26%)	3608 (2.14%)	
VI	421 (4.94%)	3563 (2.11%)	
GSC class <sup>a</sup>			0.52
GSC-benign	5443 (69.54%)	111,750 (69.18%)	
GSC-suspicious	2385 (30.46%)	49,779 (30.82%)	

(x, y) includes the nodules  $\geq x$  and  $< y$  cm.

<sup>a</sup>within Bethesda III/IV.

GSC, genomic sequencing classifier; IQR, inter quartile range.

EnrichmentMap<sup>20</sup> and Cytoscape tools<sup>21</sup> were used to build and visualize a network of significantly enriched pathways. Upregulated genes in isthmus nodules were enriched with cell migration, blood vessel development, and angiogenesis gene sets, and rRNA processing (Fig. 3, Supplementary Table S1). Upregulated genes in lobar nodules were enriched with immune system response, immune cell activation, cytokine signaling, antigen receptor-mediated signaling, and inflammatory response pathways (Fig. 3, Supplementary Table S1). To further gain insights into the immune content, we applied the ESTIMATE algorithm, which showed that isthmus nodules have lower immune content relative to lobar nodules (OR: 0.74,  $p < 0.001$ ).<sup>22</sup> Enrichment analysis and ESTIMATE results provide strong evidence of the immune coldness of isthmus tumors.

Finally, we characterized the molecular differences between thyroid isthmus and lobar carcinomas by histological subtype (PTC [isthmus = 37, lobe = 352] and IF-PTC [isthmus = 13, lobe = 181]). (Table 3). Isthmic IF-PTC had higher scores of BRS, ERK, and FMT activity relative to the lobar IF-PTCs (Fig. 4). Isthmic PTC, on the contrary, did not differ from lobar PTC, except for FMT. Isthmic PTC had higher ERK, FMT, and BRS scores relative to isthmus IF-PTC ( $p < 0.006$  for all). Within thyroid cancers that had indeterminate cytology, there was no difference between isthmus versus lobar IF-PTC nor between isthmus versus lobar PTC (Supplementary Figure S3). In terms of clinical outcomes, a cohort of 454 samples from Memorial Healthcare System (Fig. 1) with 41 isthmus nodules was analyzed. These included 9 isthmus IF-PTC and 30 isthmus PTC as well as 2 other isthmus tumor types (1 oncocytic cell carcinoma, 1 follicular thyroid carcinoma). From the 41 isthmus cancers, 32 (77%) tumors were ATA low risk, 7 (18%) were ATA intermediate risk, and 2 (5%) were ATA high risk. There was no difference in the

rates of vascular or capsular invasion, extrathyroidal extension, positive surgical margins, or lymph node metastases by cancer location.

## Discussion

In the present study, we have investigated the cytological and molecular differences between thyroid nodules and cancers arising from the isthmus as compared with the thyroid lobes. We have shown that for thyroid nodules sent for Afirma molecular testing, there is a higher rate of BV–VI cytology in isthmus nodules relative to the lobes. In addition, isthmus nodules harbor higher rates of *BRAF*-like molecular signatures and other molecular markers associated with aggressive behavior compared with those found in the lobes. Of uncertain significance is the increased frequency of *SPOP* variants found in isthmus tumors relative to those in the lobes. *SPOP* has been shown to be relatively enriched in benign thyroid nodules and was demonstrated to be a candidate alteration in “driver negative” thyroid carcinoma.<sup>23,24</sup> Interestingly, in terms of isthmus carcinomas, IF-PTC of the isthmus showed significantly higher levels of *BRAF*-like, ERK, and FMT expression scores than those of the lobes and were molecularly closer to classical PTC. Classical PTC, however, did not show molecular differences between the isthmus and the lobes except for higher rates of FMT in the isthmus locations.

Thyroid cancer is predominantly an ERK-driven carcinoma with *BRAF*<sub>p.V600E</sub> mutations found in up to 60% of PTC, followed by mutations in the different RAS isoforms (10–15%).<sup>25</sup> *BRAF* mutations lead to higher ERK activation, which may drive EMT, leading to cancer progression, metastasis, and resistance to radioiodine.<sup>26</sup> Activation of EMT has been shown to play a key role in thyroid cancer progression

TABLE 2. KEY GENOMIC ALTERATIONS FOUND IN ISTHMUS AND LOBAR NODULES IN AFIRMADB SAMPLES EXCLUDING GSC-BENIGN

	Bethesda III/IV GSC-S and bethesda V/VI			Bethesda III/IV GSC-S nodules			Bethesda V/VI nodules		
	Isthmus	Lobar	p value*	Isthmus	Lobar	p value*	Isthmus	Lobar	p value*
Total Alterations	3084	56,950		2385	49,779		699	7171	
overrepresented									
in Isthmus									
<i>BRAFp.V600E</i> variant	649 (21%)	6012 (10.6%)	<0.0001	237 (9.94%)	2571 (5.16%)	<0.0001	412 (58.9%)	3441 (48%)	<0.0001
<i>ALK/NTRK/RET</i> fusions	140 (4.54%)	1442 (2.53%)	<0.0001	102 (4.28%)	1033 (2.07%)	<0.0001	38 (5.44%)	409 (5.7%)	0.83
<i>NTRK</i> fusions	69 (2.24%)	683 (1.2%)	<0.0001	57 (2.39%)	556 (1.11%)	<0.0001	12 (1.72%)	127 (1.77%)	1
<i>RET</i> fusions	61 (1.98%)	616 (1.08%)	<0.0001	36 (1.51%)	360 (0.72%)	<0.0001	26 (3.72%)	256 (3.57%)	1
<i>SPOP</i> variants	47 (1.52%)	430 (0.76%)	<0.0001	41 (1.72%)	391 (0.78%)	<0.0001	6 (0.86%)	39 (0.54%)	0.43
Alterations									
underrepresented									
in Isthmus									
<i>NRAS</i> variants	242 (7.85%)	7499 (13.17%)	<0.0001	235 (9.85%)	7361 (14.79%)	<0.0001	7 (1%)	138 (1.92%)	0.11
<i>HRAS</i> variants	141 (4.57%)	4729 (8.3%)	<0.0001	136 (5.7%)	4643 (9.32%)	<0.0001	5 (0.72%)	86 (1.2%)	0.33
<i>PAX8::PPARG</i> fusion	33 (1.07%)	1281 (2.25%)	<0.0001	33 (1.38%)	1252 (2.51%)	<0.0001	0	29 (0.4%)	0.17
<i>RET</i> variants	2 (0.06%)	299 (0.53%)	0.001	2 (0.08%)	230 (0.46%)	0.01	0	69 (0.96%)	0.01
Alterations equally									
represented									
<i>KRAS</i> variants	52 (1.68%)	1073 (1.88%)	0.62	48 (2.01%)	1017 (2.04%)	1	4 (0.57%)	56 (0.78%)	0.7
<i>DICER1</i> variants	41 (1.33%)	702 (1.23%)	0.74	38 (1.59%)	685 (1.38%)	0.56	3 (0.43%)	17 (0.23%)	0.57
<i>TSHR</i> variants	30 (0.97%)	541 (0.95%)	0.97	26 (1.09%)	472 (0.95%)	0.67	4 (0.57%)	69 (0.96%)	0.41
<i>BRAFp.K601E</i> variant	24 (0.78%)	577 (1.01%)	0.35	24 (1%)	571 (1.14%)	0.67	0	6 (0.08%)	0.96
<i>ALK</i> fusions	10 (0.32%)	143 (0.25%)	0.66	9 (0.38%)	118 (0.24%)	0.43	1 (0.14%)	25 (0.35%)	0.57
<i>BRAF</i> fusions	22 (0.71%)	350 (0.61%)	0.66	13 (0.55%)	266 (0.53%)	1	9 (1.29%)	84 (1.17%)	0.92
<i>EIF1AX</i> variants	10 (0.32%)	129 (0.23%)	0.52	9 (0.38%)	123 (0.24%)	0.43	1 (0.14%)	6 (0.08%)	1

\*p values adjusted for multiple testing using Benjamin-Hochberg method.  
GSC-S, Genomic sequencing classifier-suspicious; IF-PTC, infiltrative follicular subtype of PTC; PTC, papillary thyroid cancer.

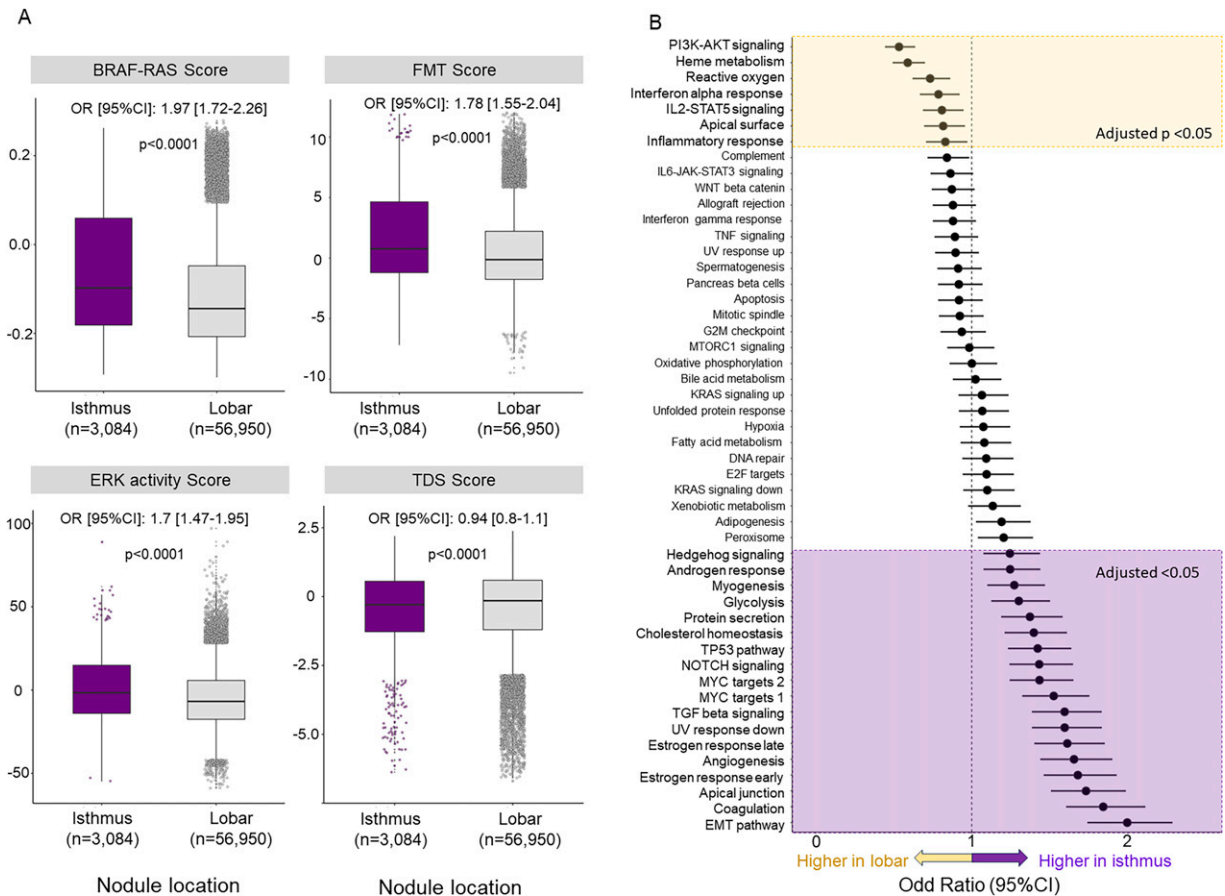


**FIG. 2.** Molecular differences between isthmus and lobar nodules. **(A)** Boxplots of key thyroid cancer molecular signatures showing higher activity of *BRAF*-RAS score, FMT, and ERK activity in isthmus nodules relative to lobar in ITN GSC-S or B V/VI samples.  $p$  Values were calculated from Wilcoxon test and adjusted with BH method and odd ratios (ORs) were calculated using logistic regression. **(B)** ORs of MSIGDB hallmark of cancer pathways and their associations with isthmus nodules (reference: lobar nodules). Samples with high EMT, coagulation, apical junction pathways were more enriched with isthmus nodules and less enriched in high PI3K-AKT, immune pathways. ORs and  $p$  values here were calculated from logistic regression and adjusted for multiple testing using BH method. BH, Benjamini-Hochberg; EMT, epithelial mesenchymal transition; FMT, follicular mesenchymal transition scores; ITN, indeterminate thyroid nodules; MSIGDB, Molecular Signatures Database.

by promoting capsular invasion, extrathyroidal extension, and both local and distant metastasis.<sup>27</sup> In this study, FMT reflects EMT specifically assessed in thyroid follicular cells.

A recent study by Alqahtani et al. evaluating nodules with BIII cytology redemonstrated a higher risk of malignancy (ROM) for isthmus nodules (66%) compared with those in the lobes (overall 48% ROM).<sup>28</sup> The majority of ITN sent for Afirma testing have BIII cytology, and it is notable there was no significant difference between the benign and suspicious result for Afirma tested ITN at the isthmus versus the lobes. There is no clear explanation for this discordance, though it may be due to a significant difference in the prevalence of cancer in BIII cytology where the Alqahtani study had a 47% ROM as compared with 13–30% expected in the United States.<sup>11</sup>

In terms of tumor behavior, Wang et al. showed that isthmus PTC had greater minimal and gross extrathyroidal extension compared with PTC from the lobes.<sup>29</sup> These clinical findings are consistent with the molecular differences of isthmus cancers compared with those arising from the lobes, such as *BRAF*-like and ERK differences. In the current

analysis, there was no significant difference in isthmus versus lobe thyroid cancer histology though this is most likely driven by the low number of isthmus cancers analyzed. This low number limits the ability to determine if the molecular differences described between isthmus and lobar tumors alters the performance of Afirma based on nodule location. The extent of surgical resection for PTCs located in the isthmus has remained a matter of considerable debate. At present, there is no standard surgical approach when treating PTC located predominantly in the isthmus.<sup>30–32</sup> The molecular findings described in this study suggest clinicians should carefully assess for aggressive clinical features in isthmus tumors, though a lack of documented long term oncologic outcomes with different surgical approaches to isthmus thyroid carcinomas tempers any clear surgical recommendation.

This study expands upon the work of Smith et al., which studied isthmus PTC, by including follicular lesions which are enriched in BIII and IV cytology as well as IF-PTC. In addition, this study analyzes molecular data from preoperative samples via the AfirmaDB, including the Afirma Xpression Atlas, though it is limited by the lack of *TERT* promoter

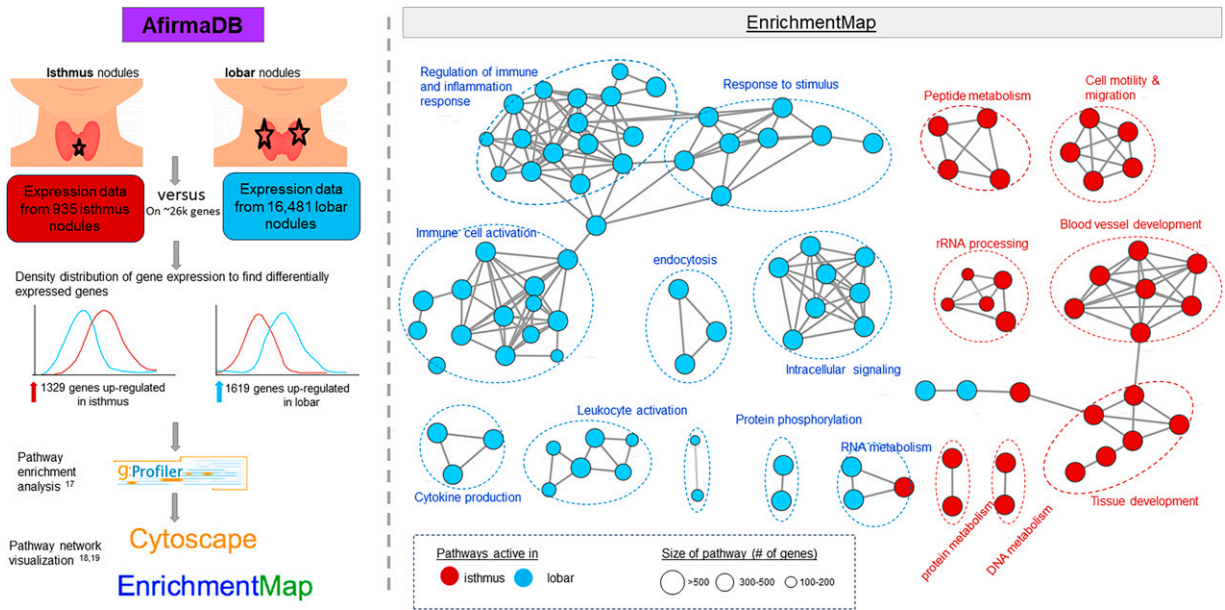


**FIG. 3.** Genome-wide differential expression analysis and Enrichmentmap of biological pathways enriched in genes upregulated in isthmus or lobar nodules. Within ITN GSC-S or Bethesda V/VI nodules, gene expression in isthmus nodules ( $n = 935$ ) was compared with lobar nodules ( $n = 16,481$ ) showing 1329 gene upregulated in isthmus and 1619 upregulated in lobar (adjusted  $p$  value  $<0.0001$ ). Gprofiler online tool was used to identify enriched biological pathways and gene sets. Enrichmentmap and cytoscape were used to build network of pathways, where every node represents a significantly enriched pathway ( $p < 0.000001$ ) and each edge represent gene overlapping between pathways. Groups of related pathways were annotated by the common pathway theme. ITN, indeterminate thyroid nodules.

mutation testing which was not available until more recently. Finally, this work is strengthened by the incorporation of features of the tumor microenvironment and immune scores via the ESTIMATE algorithm that are novel compared with other studies of isthmus thyroid tumors. Consistent with the findings of Wang et al. where PTC had lower stromal and immune scores of PTC as compared with normal thyroid,

this work leverages exome-enriched RNA-seq to show the relative immune coldness of isthmus nodules that may be a factor in the reported clinical behavior of isthmus thyroid carcinomas.<sup>33</sup>

This study is constrained by an inability to account for potential selection bias for sending isthmus tumors for molecular testing and only performing analysis of the subset

**TABLE 3.** CHARACTERISTICS OF SAMPLES WITH HISTOLOGY REPORTS USED FOR MOLECULAR ASSESSMENT OF ISTHMIC NODULES

	IF-PTC			PTC		
	Isthmus	Lobar	p value	Isthmus	Lobar	p value
Total	13	181		37	352	
Age (median [IQR])	56 (50–59)	51 (38–63)	0.4	48 (39–57)	48 (37–57)	0.7
Sex			0.18			0.22
Male	1 (7.7%)	43 (23.8%)		5 (13.5%)	78 (22.2%)	
Female	12 (92.3%)	138 (76.2%)		32 (86.5%)	274 (77.8%)	
Alterations						
<i>BRAF</i> <sup>V600E</sup> variant	5 (38.5%)	8 (4.42%)	$<0.0001$	20 (54%)	148 (42%)	0.16
<i>NRAS</i> variants	0	13 (7.18%)		1 (2.7%)	4 (1.1%)	
<i>HRAS</i> variants	0	6 (3.31%)		0	1 (0.3%)	
<i>ALK/NTRK/RET</i> fusions	0	2 (1.1%)		1 (2.7%)	12 (3.4%)	
<i>PAX8::PPARG</i> fusion	0	3 (1.65%)		0	0	
Bethesda			0.001			0.27
III	2 (15.4%)	98 (54.1%)		8 (21.6%)	83 (23.6%)	
IV	4 (30.8%)	52 (28.7%)		1 (2.7%)	30 (8.5%)	
V	1 (7.7%)	17 (9.4%)		4 (10.8%)	63 (17.9%)	
VI	6 (46.1%)	14 (7.7%)		24 (64.9%)	176 (50%)	
Tumor size (cm) (mean)	1.48	2.68	0.01	1.27	1.7	0.03

IQR, interquartile range; IF-PTC, infiltrative follicular subtype of PTC; PTC, papillary thyroid cancer.



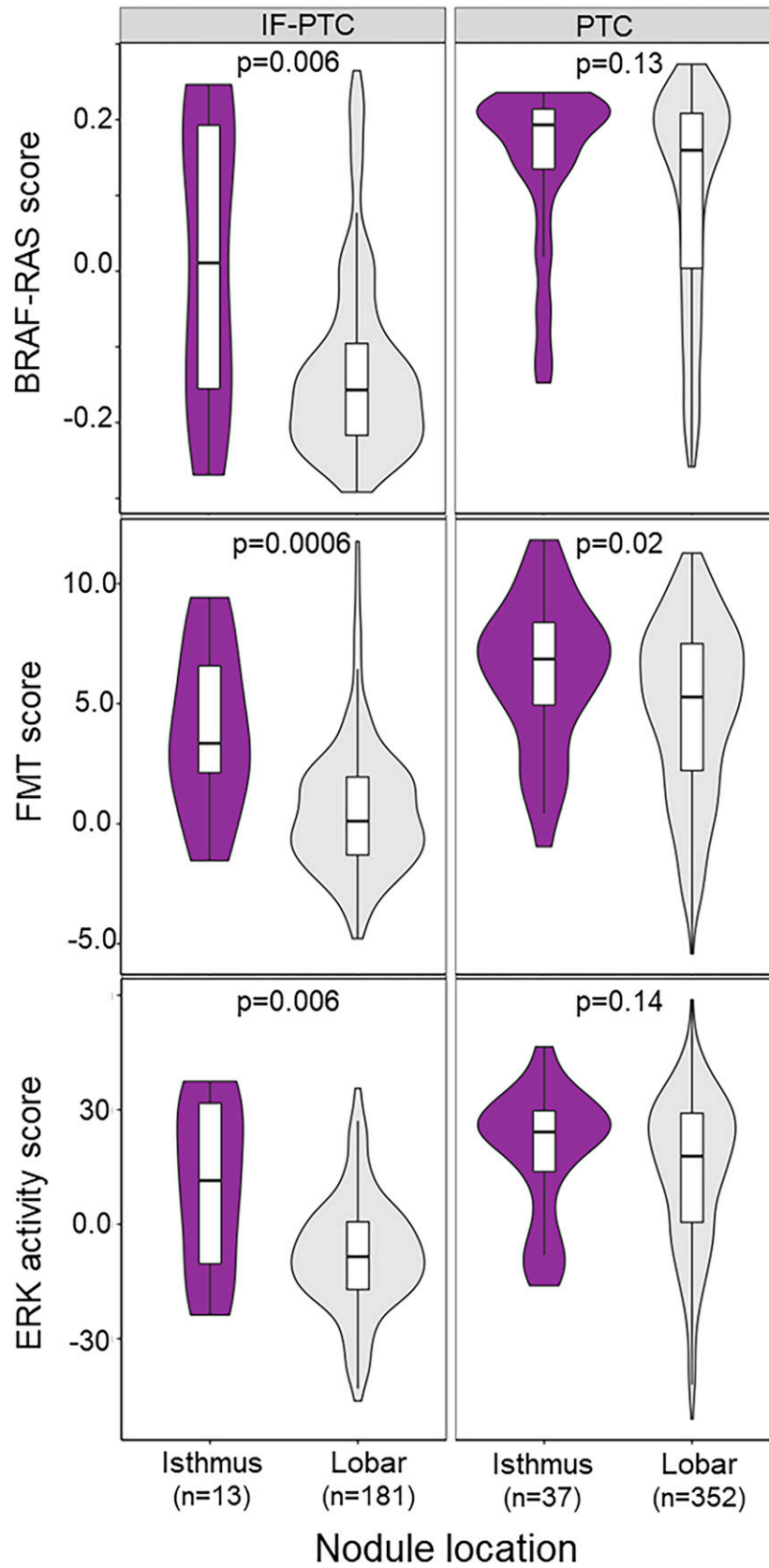


**FIG. 4.** Violin plots of thyroid molecular signatures scores across nodule locations in IF-PTC or PTC nodules showing that *BRAF-RAS* score, FMT, ERK scores are higher in isthmic IF-PTC relative to lobar IF-PTC. IF-PTC, infiltrative follicular subtype of PTC; PTC, papillary thyroid cancer.



of tumors with actionable Afirma or cytology results (GSC-S or BV–VI nodules). The relatively small number of isthmus carcinomas limits the analysis of clinical behavior differences from lobar thyroid cancers though this is consistent with the reported rates of DTC located in the isthmus that range from 1% to 9.2% for all malignant thyroid nodules.<sup>2</sup> In addition, long-term oncologic outcomes are not assessed. These hypothesis generating results indicate that future studies comparing progression free and overall survival from larger cohorts would be of interest. In addition, analyses that explore why thyroid isthmus lesions have a different molecular profile compared with lobar lesions will be valuable. In summary, isthmus thyroid nodules and IF-PTC of the isthmus appear to be cytologically and molecularly more aggressive than those of the thyroid lobes. More data are needed to know if a change in surgical therapy is warranted in isthmus thyroid cancers relative to lobar cancers and if this molecular data should influence isthmus thyroid tumor management and monitoring.

### Authors' Contributions

S.J. and T.C.B. conceptualized the study and helped with article preparation and review. A.G. and D.B. provided clinical data and reviewed the article. J.P.K., M.A., and R.T.K. helped with study design and article preparation and review. M.A., R.J., Y.C., Y.H., and J.H. helped with data analysis, article preparation, and review. All authors reviewed the final article, and all gave final approval for publication.

### Author Disclosure Statement

M.A., R.J., Y.C., Y.H., J.H., J.P.K., and R.T.K. are employees and equity owners of Veracyte, Inc. S.J., T.C.B., A.G., and D.B. have no disclosures.

### Funding Information

There was no external funding source for this project.

### Supplementary Material

Supplementary Figure S1  
 Supplementary Figure S2  
 Supplementary Figure S3  
 Supplementary Table S1

### References

- Haugen BR, Alexander EK, Bible KC, et al. 2015 American Thyroid Association management guidelines for adult patients with thyroid nodules and differentiated thyroid cancer: The American Thyroid Association guidelines task force on thyroid nodules and differentiated thyroid cancer. *Thyroid* 2016;26(1):1–133; doi: 10.1089/thy.2015.0020
- Jasim S, Baranski TJ, Teefey SA, et al. Investigating the effect of thyroid nodule location on the risk of thyroid cancer. *Thyroid* 2020;30(3):401–407; doi: 10.1089/thy.2019.0478
- Pastorello R, Valerio E, Lobo A, et al. Do thyroid nodules that arise in the isthmus have a higher risk of malignancy? *Cancer Cytopathol* 2020;128(8):520–522; doi: 10.1002/cncy.22260
- Luo H, Yan F, Lan L, et al. Ultrasonographic features, nodule size, capsular invasion, and lymph node metastasis of solitary papillary carcinoma of Thyroid Isthmus. *Front Oncol* 2020;10:558363; doi: 10.3389/fonc.2020.558363
- Hahn SY, Han BK, Ko EY, et al. Ultrasound findings of papillary thyroid carcinoma originating in the isthmus: Comparison with lobe-originating papillary thyroid carcinoma. *Am J Roentgenol* 2014;203(3):637–642; doi: 10.2214/AJR.13.10746
- Song CM, Lee DW, Ji YB, et al. Frequency and pattern of central lymph node metastasis in papillary carcinoma of the thyroid isthmus. *Head Neck* 2016;38 Suppl 1:E412–E416; doi: 10.1002/hed.24009
- Santrac N, Besic N, Buta M, et al. Lymphatic drainage, regional metastases and surgical management of papillary thyroid carcinoma arising in pyramidal lobe—a single institution experience. *Endocr J* 2014;61(1):55–59; doi: 10.1507/endocrj.ej13-0316
- Zhou L, Gao C, Li H, et al. Isthmic papillary thyroid carcinoma presents a unique pattern of central lymph node metastasis. *Cancer Manag Res* 2020;12:3643–3650; doi: 10.2147/CMAR.S252692
- Smith ER, Frye CC, Pandian TK, et al. Molecular characteristics of isthmus papillary thyroid cancers: Supporting evidence for unfavorable clinical behavior. *Am J Surg* 2024; 228:146–150; doi: 10.1016/j.amjsurg.2023.09.005
- Bongiovanni M, Spitale A, Faquin WC, et al. The Bethesda system for reporting thyroid cytopathology: A meta-analysis. *Acta Cytol* 2012;56(4):333–339; doi: 10.1159/000339959
- Ali SZ, Baloch ZW, Cochand-Priollet B, et al. The 2023 Bethesda system for reporting thyroid cytopathology. *Thyroid* 2023;33(9):1039–1044; doi: 10.1089/thy.2023.0141
- Alexander EK, Kennedy GC, Baloch ZW, et al. Preoperative diagnosis of benign thyroid nodules with indeterminate cytology. *N Engl J Med* 2012;367(8):705–715; doi: 10.1056/NEJMoa1203208
- Patel KN, Angell TE, Babiarz J, et al. Performance of a genomic sequencing classifier for the preoperative diagnosis of cytologically indeterminate thyroid nodules. *JAMA Surg* 2018;153(9):817–824; doi: 10.1001/jamasurg.2018.1153
- Walsh PS, Hao Y, Ding J, et al. Maximizing small biopsy patient samples: Unified RNA-Seq platform assessment of over 120,000 patient Biopsies. *J Pers Med* 2022;13(1):24; doi: 10.3390/jpm13010024
- Ladenson PW, Klopper JP, Hao Y, et al. Combined Afirma genomic sequencing classifier and TERT promoter mutation detection in molecular assessment of Bethesda III–VI thyroid nodules. *Cancer Cytopathol* 2023;131(10):609–613; doi: 10.1002/cncy.22744
- Hu MI, Waguespack SG, Dosiou C, et al. Afirma genomic sequencing classifier and Xpression atlas molecular findings in consecutive Bethesda III–VI thyroid nodules. *J Clin Endocrinol Metab* 2021;106(8):2198–2207; doi: 10.1210/clinem/dgab304
- Angell TE, Wirth LJ, Cabanillas ME, et al. Analytical and clinical validation of expressed variants and fusions from the whole transcriptome of thyroid FNA Samples. *Front Endocrinol (Lausanne)* 2019;10:612; doi: 10.3389/fendo.2019.00612
- Liberzon A, Birger C, Thorvaldsdottir H, et al. The Molecular Signatures Database (MSigDB) hallmark gene set collection. *Cell Syst* 2015;1(6):417–425; doi: 10.1016/j.cels.2015.12.004

19. Kolberg L, Raudvere U, Kuzmin I, et al. g:Profiler-interop-erable web service for functional enrichment analysis and gene identifier mapping (2023 update). *Nucleic Acids Res* 2023;51(W1):W207–W212; doi: 10.1093/nar/gkad347
20. Merico D, Isserlin R, Stueker O, et al. Enrichment map: A network-based method for gene-set enrichment visualization and interpretation. *PLoS One* 2010;5(11):e13984; doi: 10.1371/journal.pone.0013984
21. Shannon P, Markiel A, Ozier O, et al. Cytoscape: A software environment for integrated models of biomolecular interaction networks. *Genome Res* 2003;13(11):2498–2504; doi: 10.1101/gr.1239303
22. Yoshihara K, Shahmoradgoli M, Martinez E, et al. Inferring tumour purity and stromal and immune cell admixture from expression data. *Nat Commun* 2013;4:2612; doi: 10.1038/ncomms3612
23. Ye L, Zhou X, Huang F, et al. The genetic landscape of benign thyroid nodules revealed by whole exome and transcriptome sequencing. *Nat Commun* 2017;8:15533; doi: 10.1038/ncomms15533
24. Bim LV, Carneiro TNR, Buzatto VC, et al. Molecular signature expands the landscape of driver negative thyroid cancers. *Cancers (Basel)* 2021;13(20); doi: 10.3390/cancers13205184
25. Cancer Genome Atlas Research Network. Integrated genomic characterization of papillary thyroid carcinoma. *Cell* 2014; 159(3):676–690; doi: 10.1016/j.cell.2014.09.050
26. Xing M. Molecular pathogenesis and mechanisms of thyroid cancer. *Nat Rev Cancer* 2013;13(3):184–199; doi: 10.1038/nrc3431
27. Shakib H, Rajabi S, Dehghan MH, et al. Epithelial-to-mesenchymal transition in thyroid cancer: A comprehensive review. *Endocrine* 2019;66(3):435–455; doi: 10.1007/s12020-019-02030-8
28. Alqahtani SM, Altalhi BA, Alalawi YS, et al. Is the nodule location a predictive risk factor for cancer in AUS/FLUS thyroid nodules? A Retrospective Cohort Study. *Asian J Surg* 2024;47(6):2574–2578; doi: 10.1016/j.asjsur.2024.02.096
29. Wang H, Zhao S, Yao J, et al. Factors influencing extrathyroidal extension of papillary thyroid cancer and evaluation of ultrasonography for its diagnosis: A retrospective analysis. *Sci Rep* 2023;13(1):18344; doi: 10.1038/s41598-023-45642-x
30. Vasileiadis I, Boutzios G, Karalaki M, et al. Papillary thyroid carcinoma of the isthmus: Total thyroidectomy or isthmusectomy? *Am J Surg* 2018;216(1):135–139; doi: 10.1016/j.amjsurg.2017.09.008
31. Park H, Harries V, McGill MR, et al. Isthmusectomy in selected patients with well-differentiated thyroid carcinoma. *Head Neck* 2020;42(1):43–49; doi: 10.1002/hed.25968
32. Gui Z, Wang Z, Xiang J, et al. Comparison of outcomes following thyroid isthmusectomy, unilateral thyroid lobectomy, and total thyroidectomy in patients with papillary thyroid microcarcinoma of the Thyroid Isthmus: A Retrospective Study at a Single Center. *Med Sci Monit* 2020;26:e927407; doi: 10.12659/MSM.927407
33. Wang Y, He Y, Cao L, et al. Exploring the correlation analysis of immune microenvironment, mutation burden and prognosis of papillary thyroid carcinoma based on Estimate algorithm. *Gland Surg* 2022;11(5):860–867; doi: 10.21037/gs-22-211

Address correspondence to:  
*Joshua P. Klopper, MD*  
*Veracyte, Inc.*  
*6000 Shoreline Ct.*  
*Suite 300*  
*South San Francisco*  
*CA 94080*  
*USA*

*E-mail: Joshua.klopper@veracyte.com*